

Can global warming affect tropical ocean heat transport?

Wilco Hazeleger

Royal Netherlands Meteorological Institute (KNMI), de Bilt, The

Netherlands

Dr. W. Hazeleger, Oceanographic Research, KNMI, PO Box 201, 3730 AE, de Bilt, The Netherlands. (Wilco.Hazeleger@knmi.nl)

Tropical meridional ocean heat transport is studied in six coupled ocean-atmosphere models in which atmospheric CO₂ concentration has been increased. In the Indo-Pacific, the strength of Subtropical Cells (STCs) changes in response to changes in the trade winds. However, the change is not consistent among models. In contrast, in all models the tropical Indo-Pacific heat transport remains nearly constant over time due to compensation of STC and the horizontal gyre variations. Even under strong atmospheric radiative forcing the tropical Indo-Pacific ocean heat transport trends are determined by changes in circulation, rather than changes in the stratification. Ocean heat transport in the tropical Atlantic responds to weakening of the basin-wide meridional overturning circulation (MOC). The trends in the South Atlantic STC do not affect ocean heat transport.

1. Introduction

Meridional energy transport mediates the imbalance between incoming radiation at the top of the atmosphere and outgoing long wave radiation. In the tropics, the ocean transfers most heat poleward. Elsewhere, the atmosphere dominates, although in the North Atlantic the ocean heat transport is significant as well [*Trenberth and Caron, 2001*].

Changes in poleward ocean heat transport (OHT) are often related to changes in the oceanic overturning cells. In particular, the basin-wide meridional overturning circulation (MOC) in the Atlantic may weaken in response to warming and freshening in the Arctic in response to rising greenhouse gas concentrations in the atmosphere [*Cubasch et al. 2001*]. Changes in Subtropical Cells [STCs, *McCreary and Lu 1994*] in response to global warming have hardly been studied, but *Merryfield and Boer [2004]* report a weakening of the STCs in a coupled ocean-atmosphere model.

Some conceptual models indicate that energy transport changes in the ocean and atmosphere in the tropics act in concert [*Held 2001*]. This is based on the tight constraint between transport by the Hadley Cells and STCs, both of which are determined by momentum transfer between ocean and atmosphere. However, *Hazeleger et al. [2004]* showed that the gyre heat transport can compensate substantially for changes in OHT by STCs. In contrast, radiative constraints would require that oceanic and atmospheric heat transport compensate [*Bjerknes 1964*]. However, trends in outgoing longwave radiation at the top of the atmosphere indicate that in a transient climate the partitioning can change [*Wielicki et al. 2002*].

Here we study how tropical oceanic overturning cells and meridional OHT can change when the climate changes due to rising greenhouse gasses. Previous studies focused on seasonal to decadal time scales at which the tropical dynamics is primarily wind-driven. Here we study long-term trends in global coupled ocean-atmosphere models. The models were run with the same external forcing but differ significantly in model formulation.

2. Models and experiments

Output of state-of-the-art global coupled ocean-atmosphere models are used that were compiled for the assessment of climate change by the *Intergovernmental Panel on Climate Change* (IPCC). The models that are used here have been initialized from an equilibrated state that was obtained after a spinup with atmospheric composition for the year 1850. Subsequently atmospheric CO₂ concentration was changed by one percent per year up to quadrupling of the CO₂ concentration (after 140 years) and stabilizing afterward. Some experiments were integrated up to doubling of CO₂ concentration. The quadrupling of CO₂ experiments are used as we are looking for substantial variations in OHT. Output from six coupled models was available for analysis (see Table 1). Annual data have been used, except when calculating the different components of OHT for which case monthly data have been used. In some models a non-zero overturning strength at the surface reflects changes in the Bering Strait transport when the overturning strength is referenced to zero at the bottom. In those cases, a net barotropic transport correction has been applied through each basin corresponding to the net Bering Strait transport. Also, care must be taken when interpreting OHT in open basins as results depend on the temperature scales. Since heat transport through the Bering Strait is very small

and contains small trends, this hardly affects the results. The CNRM-CM3 model and the GISS-ER model use a temperature scale in Celsius, the MIROC3.2-medres model uses potential temperature in Celsius (referenced to the surface). The MRI-CGCM2.3.2 calculates heat transport with a residual method using the surface heat fluxes and the change in static energy.

3. Results

3.1. Changes in Atlantic overturning cells

In response to changes in the surface heat flux and to changes in the surface water flux the basin-wide MOC in the Atlantic reduces in strength in most coupled ocean-atmosphere models [*Cubasch et al.* 2001]. The new model simulations show similar behavior (Figure 1a), in accordance with the results of *Gregory et al.* [2005]. Only the MRI-CGCM2.3.2 model shows hardly any change. The spatial structure of the trends displays much bigger differences among the runs than do the time series of maximum overturning strength. Two extreme model solutions are presented in Figure 2. As we focus on the tropical OHT, the mean and change of overturning circulation in the upper ocean are shown. The MRI-CGCM2.3.2 model shows a slight increase of the overturning circulation in the upper Atlantic (Figure 2a). The trend has a much different structure than the mean overturning in the upper ocean. In the deeper layers a shoaling of the MOC is found (not shown). In contrast, the GISS-ER model (Figure 2c) shows a reduction of the overturning.

In all models an STC is present in the South Atlantic. This STC is primarily driven by Ekman divergence at the equator and subduction in the subtropical oceans. In the Atlantic the northern STC is hardly distinguishable in zonally averaged fields due to

the dominance of the MOC. Streamlines can close upon themselves close to the equator with downwelling at 5°N (the "tropical cell"), but the zonally integrated Eulerian time-mean circulation does not seem to ventilate the equatorial thermocline from the northern subtropics in any of the models studied here.

When the MOC reduces, the interhemispheric transport decreases as well. However, this hardly affects the magnitude of the South Atlantic STC in most models (Figure 1b). Figure 2a and c illustrate that the major changes in overturning strength are found below the STCs and reflect changes in the upper limb of the MOC.

3.2. Changes in Indo-Pacific overturning cells

Due to the presence of the Indonesian Throughflow, the Pacific and Indian Ocean will be considered together. The models analyzed here differ significantly in simulated STC strength (Figure 1c), structure and trends (Figure 2b,d). In general these trends occur in the upper Indo-Pacific only, suggesting wind-driven mechanisms. Indeed, the trends are related to changes in Hadley Cell strength in the respective atmospheric components of the coupled models (C.M. Mitas and A. Clement, pers. comm.), such that when the Hadley Cell reduces the Subtropical Cell strength reduces and vice versa. Similar changes are found in the southern hemisphere (not shown). The transport time series show substantial decadal variability, which must be the result of intrinsic variations in the Indo-Pacific. However, this variability is smaller than the variability observed in the 1990s [McPhaden and Zhang 2004] indicating the weak decadal El Niño-like variability in the models. The implications for OHT are discussed in next section.

3.3. Changes in ocean heat transport

The ocean heat transport is defined as $OHT = \rho_w c_p \int_L \int_H v T dz dx$, with v the meridional velocity, T the temperature, ρ_w the density of sea water, c_p the heat capacity of sea water, H the depth, and L the width of the basin. Zonally closed basins are used. In the North Atlantic, the reduction of the MOC leads to a reduction of OHT (Figure 1d). The sensitivity of OHT change to overturning change is similar in all models: 0.035 ± 0.006 PW/Sv; the error is the standard deviation of the sensitivity obtained by linear regression between the runs.

OHT changes in the tropical and South Atlantic (Figure 1e) are of the same order of magnitude as in the North Atlantic. However, these changes do not correlate well with trends in amplitude of the South Atlantic STC. The changes in OHT are primarily dictated by changes in the MOC (see section 3.4).

In the Indo-Pacific, the STCs change, but the sign is not consistent among models. Surprisingly, OHT in nearly all models hardly changes, although it contains decadal variations (Figure 1f). The insensitivity of OHT to STC trends is found in the southern tropical Indo-Pacific as well (not shown). Only the coarse resolution GISS-ER model shows a substantial reduction of OHT. In ocean-only models the near compensation between poleward OHT by the Ekman-driven STCs and equatorward OHT by geostrophic horizontal flow can explain the small changes in the Pacific on decadal time scales [Hazeleger *et al.* 2004]. As the GISS-ER model does not resolve boundary currents well, this compensation may not occur. In the next section we study how OHT compensation by gyres and STCs holds on long time scales.

3.4. Decomposition of ocean heat transport

To discriminate between the effect of overturning cells and the horizontal gyres on meridional OHT we decompose it into:

$$\rho_w c_p [\overline{vT}] = \rho_w c_p [\overline{v}][\overline{T}] + \rho_w c_p [\overline{v^*T^*}] + \rho_w c_p [\overline{v'T'}]. \quad (1)$$

The square brackets denote the zonal average, the * denotes deviations from the zonal mean, the primes denote deviation from the time mean, and the bar denotes the time average. All terms are zonally and vertically integrated. The last term will be ignored in this study. We follow the usual conventions to call the first term on the right hand side the overturning component and the second term the gyre component.

The contrasting effects of changes in the overturning cells and horizontal gyres on changes in ocean heat transport are illustrated by the linear trends in the CNRM-CM3 model (Figure 3). The trends are obtained by ordinary least squares regression of the different OHT components in Equation 1 (these components were not available for other models). In the Atlantic, the trend of OHT at nearly all latitudes can be explained from the trend in overturning component. Also, the sum of the gyre and overturning component nearly matches the total OHT. As these terms were independently calculated, this justifies ignoring the last term in Equation 1.

In the tropical Indo-Pacific, the coupled model shows compensation between trends in the overturning component and in the gyre component resulting in small net changes in OHT. So, the response to greenhouse warming on interdecadal time scales is similar to the decadal changes found in observational data sets [McPhaden and Zhang 2004] and in models [Lee and Fukumori 2004], where compensation was found as well. The close

compensation is surprising as changes in meridional temperature gradients on long time scales would result in subduction of anomalous warm water masses, affecting the static stability of the ocean column and meridional OHT [e.g. *Hazeleger et al.* 2001, *Boccalletti et al.* 2004].

4. Conclusions

By comparing different coupled models with the same greenhouse gas increase, modeled changes in tropical OHT induced by global warming were studied. Although the response of STC strength differs between models, the relation between MOC strength, STC strength and OHT is similar in most models.

In the Atlantic, STC strength hardly changes in most models and tropical OHT follows changes in the MOC. As most models show a significant reduction of the MOC in response to global warming this leads to a reduction of heat transport in the tropical Atlantic and South Atlantic in most models. Only the MRI-CGCM2.3.2 does not show a reduction. This could be a consequence of the flux corrections used in this model.

In the tropical Indo-Pacific, wind-driven mechanisms dominate the changes in OHT. Despite changes in STC strength, the changes in OHT are relatively small due to compensation between changes in horizontal gyre heat transport and in overturning heat transport. This is surprising, as on long time scales the diabatic effects of changes in subducted water masses are expected to have an effect on tropical OHT. Apparently, the changes in temperature are rather uniform and hardly affect static stability of the ocean. The results differ from those found by *Merryfield and Boer* [2004]. Differences between models are expected as horizontal resolution affects the representation of western bound-

ary currents. A too small gyre heat transport is expected in coarse resolution models (e.g. the GISS-ER model) leaving more room for STCs to affect heat transport. The implications of these results for variations in atmospheric heat transport are unclear and will be studied in the near future.

Acknowledgments. R Seager, A Clement, C Mitas, S Drijfhout and GJ van Oldenborgh are thanked for valuable discussions. Two reviewers are thanked for constructive comments. The international modeling groups are acknowledged for providing their data for analysis, the Program for Climate Model Diagnosis and Intercomparison for collecting and archiving the model data, the JSC/CLIVAR Working Group on Coupled Modelling and their Coupled Model Intercomparison Project and Climate Simulation Panel for organizing the model data analysis activity, and the IPCC WG1 TSU for technical support. The IPCC Data Archive at Lawrence Livermore National Laboratory is supported by the Office of Science, U.S. Department of Energy.

References

- Bjerknes, J. (1964), Atlantic air/sea interaction. *Adv. Geophys.*, 10, 1-82.
- Boccaletti, G. Pacanowski R.C., Philander S.G.H., and Fedorov A.V. (2004), The Thermal Structure of the Upper Ocean. *J. Phys. Oceanogr*, 34, 888–902.
- Cubasch, U., and Coauthors (2001) Projections of future climate change, in *Climate Change 2001: The Scientific Basis*. edited by J.T. Houghton et al. pp. 525-582, Cambridge Univ. Press, New York.

- Delworth, T. L., and Coauthors (2005), GFDLs CM2 global coupled climate models Part 1: Formulation and simulation characteristics. *J. Climate*, accepted.
- Gordon, H.B. and Coauthors (2002), The CSIRO Mk3 climate system model. *CSIRO Atmospheric Research Technical Paper, No. 60*, Victoria, Australia, 130pp.
- Gregory, J. M. and Coauthors (2005), A model intercomparison of changes in the Atlantic thermohaline circulation in response to increasing atmospheric CO₂ concentration. *Geoph. Res. Lett.*, *32*, doi 10.1029/2005GL023209.
- Hazeleger, W., R. Seager, M. Visbeck, N. Naik, and K. Rodgers (2001), Impact of mid-latitude storm track on the upper Pacific Ocean. *J. Phys. Oceanogr.*, *31*, 616–636.
- Hazeleger, W., R. Seager, M. Cane, and N. Naik (2004), How can tropical Pacific ocean heat transport vary? *J. Phys. Oceanogr.*, *34*, 320–333.
- Held, I.M. (2001), The partitioning of the poleward energy transport between the tropical ocean and atmosphere. *J. Atmos. Sci.*, *58*, 943–948.
- Lee, T., and I. Fukumori (2003), Interannual-to-decadal variations of tropical-subtropical exchange in the Pacific ocean: boundary versus interior pycnocline transports. *J. Climate*, *16*, 4022-4042.
- McCreary, J. P., and P. Lu (1994), On the interaction between the subtropical and equatorial ocean circulation: the subtropical cell, *J. Phys. Oceanogr.*, *24*, 466–497.
- McPhaden M. J., and D. Zhang (2004), Pacific Ocean circulation rebounds, *Geophys. Res. Lett.*, *31*, doi:10.1029/2004GL020727.
- Merryfield W. J. and G. J. Boer (2005), Variability of Upper Pacific Ocean Overturning in a Coupled Climate Model. *J. Clim.*, *18*, 666–683.

- Schmidt, G. A., and Coauthors (2005), Present day atmospheric simulations using GISS ModelE: Comparison to in-situ, satellite and reanalysis data, *J. Climate*, accepted.
- Trenberth, K.E., and J.M. Caron (2001), Estimates of meridional atmosphere and ocean heat transports. *J. Climate*, 14, 3433-3443.
- Wielicki, B.A., and Coauthors (2002), Evidence for large decadal variability in the tropical mean radiative energy budget. *Science*, 295, 841–844.
- Yukimoto, S. and Coauthors (2001) A new MRI coupled GCM (MRI-CGCM2) model climate and its variability. *Pap. Meteor. Geophys.*, 51, 47–88.

Table 1. Coupled ocean-atmosphere models used in this study

model	atmospheric resolution	ocean resolution	reference
CNRM-CM3	T63L45	$2^{\circ} \times 0.5^{\circ}$ L31	Salas-Melia et al. (subm)
CSIRO-Mk3.0	T63L18	$1.875^{\circ} \times 0.84^{\circ}$ L31	Gordon et al. 2002
GISS-ER	$5^{\circ} \times 4^{\circ}$ L20	$5^{\circ} \times 4^{\circ}$ L13	Schmidt et al. (2005)
MIROC3.2(medres)	T42L20	$1.4^{\circ} \times 0.5^{\circ}$ L43	K1 Coupled GCM (in prep)
MRI-CGCM2.3.2	T42L30	$2.5^{\circ} \times 0.5^{\circ}$ L23	Yukimoto et al. 2001
GFDL-CM2.1	$2.5^{\circ} \times 2^{\circ}$ L24	$1^{\circ} \times 1/3^{\circ}$ L50	Delworth et al. (2005)

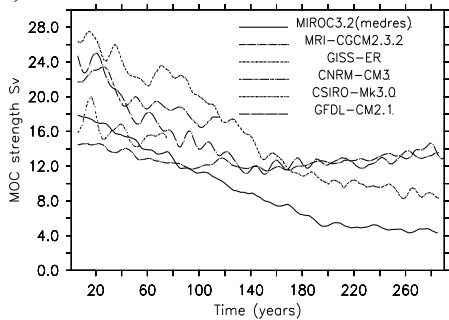
Resolutions at the equator are given (L=number of layers, T=wavenumber of spectral truncation). For the CSIRO-MK3.0 and the GFDL-CM2.1 models only overturning strengths were available. The MRI-CGCM2.3.2 model used flux corrections for heat, fresh water and tropical wind stress. Only for the CNRM-CM3 model the overturning and gyre components of OHT were available.

Figure 1. Changes in magnitude of overturning cells (top) and northward OHT (bottom). a) Maximum strength of overturning and d) maximum OHT in the North Atlantic (2°N-90°N). b) Maximum strength of overturning in the upper South Atlantic (2°S-30°S,0-400m) and e) maximum OHT in the South Atlantic. c) Maximum strength of overturning in the upper North Pacific (2°N-30°N, 0-300m) and f) maximum OHT in the North Pacific. A 10-yr filter has been applied.

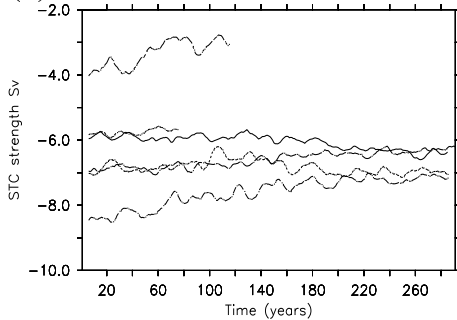
Figure 2. Mean strength (contours, average over year 1-20) and change (colors, difference between year 271-290 and year 1-20) of overturning strength in the upper Atlantic (a and c) and upper Indo-Pacific (b and d) in Sv ($=10^6\text{m}^3\text{s}^{-1}$) in the MRI-CGCM2.3.2 model (a and b) and the GISS-ER model (c and d).

Figure 3. Linear trends (PW/century) of total northward OHT, overturning OHT and gyre OHT in the CNRM-CM3 model. Top: Atlantic Ocean. Bottom: Indo-Pacific Ocean.

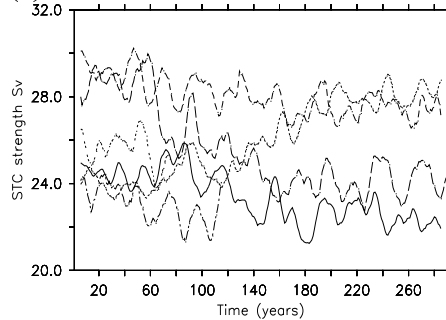
(a)



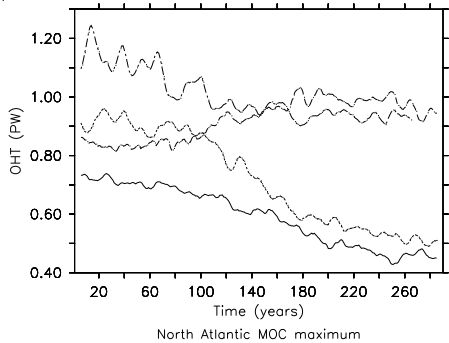
(b)



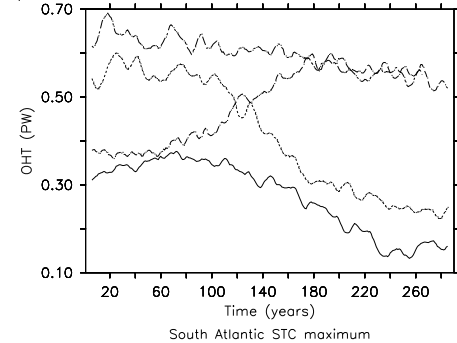
(c)



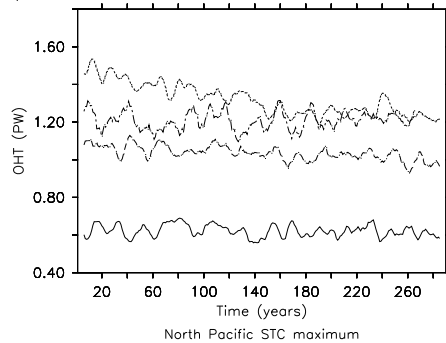
(d)

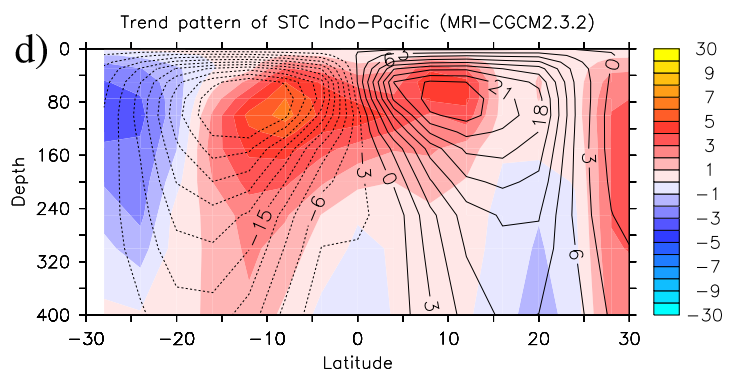
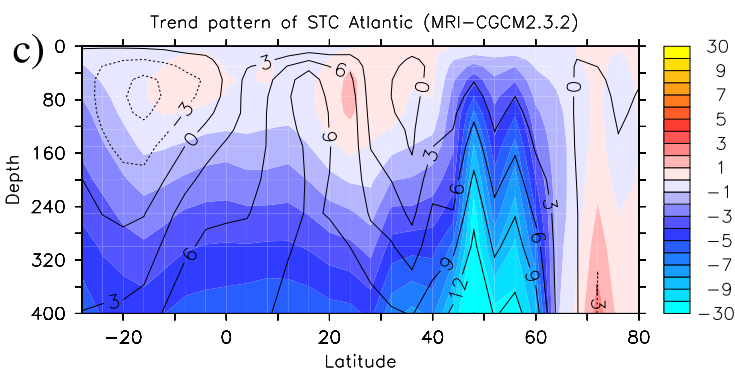
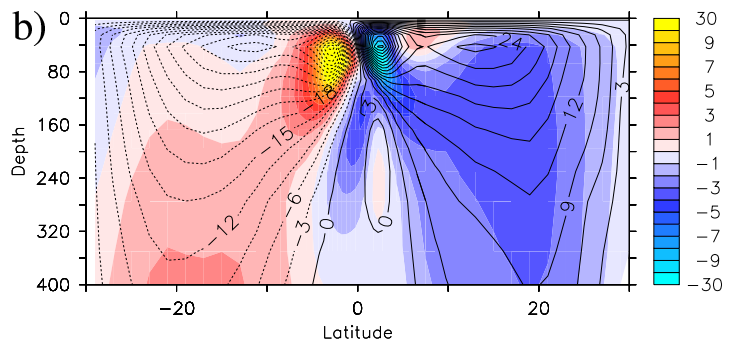
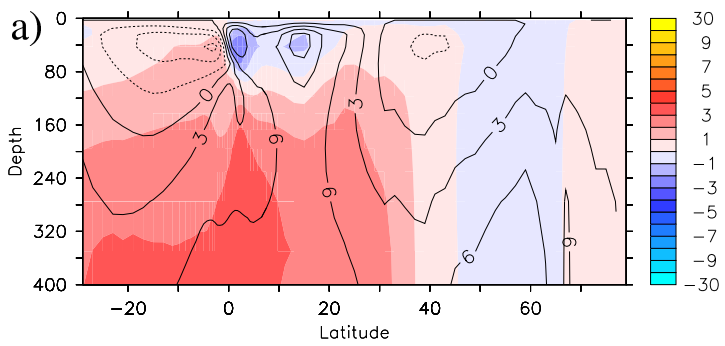


(e)



(f)





Trend pattern of STC Atlantic (GISS-ER)

Trend pattern of STC Indo-Pacific (GISS-ER)

